International Journal of Fracture (2005) 136:221–235
DOI 10.1007/s10704-005-6032-y

Field emissions caused by fracture and yielding

S.R. WINKLER
Fraunhofer-Institut für Werkstoffmechanik, Freiburg, Germany

Received 6 July 2005; accepted in revised form 20 December 2005

Abstract. Two effects, magnetic and electric emission, have been observed and used in fracture tests to detect and analyse onset and progress of plastic deformation and fracture. While magnetic emission (ME) occurs only in ferromagnetic materials, electric emission (EE) can be found with any material, metals as well as plastics, ceramics, glass, and others. In ferromagnetic materials the two effects supplement each other. In steel, for example, electric emission is produced by plastic deformation but not by fracture; magnetic emission, on the other hand, is produced by fracture but not by plastic deformation. This paper describes the effects, demonstrates their application in Charpy tests, and shows how to derive fracture parameters, for instance the instants of the onset of plastic deformation and fracture. ME and EE, therefore, yield an attractive, inexpensive and fast supplement to conventional fracture test methods.

Key words: Brittle or unstable ductile or plastic collapse, Charpy test, crack tip plastic deformation, crack velocity, electric emission, final failure, logarithmic amplification, magnetic emission, onset of stable crack growth, probe, sensor, stretch zone formation, tensile test, wave velocity.

1. Introduction

The inherent magnetic field in samples of ferromagnetic materials changes when energetic effects occur in the material, in particular when the piece of material is mechanically stressed or fractured. These field variations originally found in Barkhausen (1919) can be observed by suitable sensors and used to detect the onset, magnitude, and progress of the originating effects. The basis of the field variations is the magnetic character of the material's microstructure and the arrangement of magnetic domains according to an energy minimizing principle. Each change of energy results in a rearrangement of the magnetic structure and, consequently, in a field variation. For application in fracture mechanics this magnetic effect is labelled magnetic emission ME (Winkler, 1988) in analogy to the long known acoustic emission AE.

Not restricted to certain materials is the observation of electric fields, generated or varied in mechanically stressed materials. Molecular or structural deformations as well as charge separations in fracture experiments are responsible for this effect, labelled electric emission EE (Winkler, 1990a).

The Charpy V-notch test is a suitable experiment for investigating the two emissions, because (a) the two probes can easily be installed at the hammer in addition to the force instrumentation and no further care has to be taken for them, and (b) the entire loading and fracturing event is limited to a few distinct milliseconds, allowing easy observation and comparison with the corresponding load function. But of course there is no restriction to the Charpy test. Emission sensors can be applied also to any other fracture mechanics test.

The following two Sections, 2 and 3, briefly describe ME and EE principles and their sensors and probes. Section 4 points out the advantages of field emissions in comparison with others. Section 5 describes how the two emissions can be combined for an investigation complement. In this example of a Charpy experiment on steel important data for fracture evaluation are gained. It is shown that the total process of deformation and fracture can be monitored by these three signals: force F, ME, and EE, when also the computable integrals of the emissions, the corresponding fields, are considered.

2. Magnetic emission (ME)

Two effects compose the magnetic emission, (a) the Barkhausen noise due to energy changes in the sample and (b) the change of the magnetic field due to damage and fracture when new surfaces and voids filled with vacuum or air are inserted in the magnetic path. Reversible low level Barkhausen noise signals appear randomly positive or negative when the internal energy changes due to minor load applications. Higher level Barkhausen noise, however, and the changes due to fracture appear irreversible (Kittel, 1986). To make the second effect plausible the field H in and outside of a ferromagnetic material is considered (magnetic induction $B = \text{const.}$):

$$\vec{H} = \frac{\vec{B}}{\mu_0 \mu_r} \tag{1}$$

where $\mu_0 = 1.256\ldots \cdot 10^{-6}$ Vs $A^{-1}m^{-1}$ is the magnetic field constant and the dimensionless $\mu_r \sim 10^3$ or 10^4 is the relative material permeability for an iron material, $\mu_r = 1$ for vacuum, $\mu_r \approx 1$ for air. It is obvious that the field in the void is a thousand times or more larger than in the material. Both components affect the local field distribution, the changes of which can be picked up by a coil yielding an electric signal

$$U \propto \frac{\mathrm{d}H}{\mathrm{d}t}. \tag{2}$$

The amplitude of a magnetic signal depends on both the speed of the effect and its magnitude. If a fracture appears brittle and rapid, and the fracture area is large, the signal is large, too. If, however, fracture takes place in elementary steps, corresponding to the size of grains or inclusions or less, these elementary signals are small and hard to distinguish from normal low level Barkhausen or electronic noise. It has been tried, therefore, with some success to use a logarithmic amplification in order to separate the signals. A logarithmic amplifier works with the transfer equation

$$U_{\text{out}} = U_{\text{D}} \log \frac{|U_{\text{ME}}|}{U_0}, \tag{3}$$

where U_{D} is the voltage per decade, U_0 is the input voltage at zero out, and U_{ME} is the emission signal. In the realized amplifier's version a ± 10 V range was used for a 4 decades presentation, with $U_{\text{D}} = 5$ V and $U_0 = 10$ mV. With an output scale of 2.5 V/div the log scale is $0.1\,\text{mV} \div 1\,\text{mV} \div 10\,\text{mV} \div 100\,\text{mV} \div 1$ V for every two divisions. The principles of the logarithmic amplification are described in some detail in Winkler (1988, 1990b).

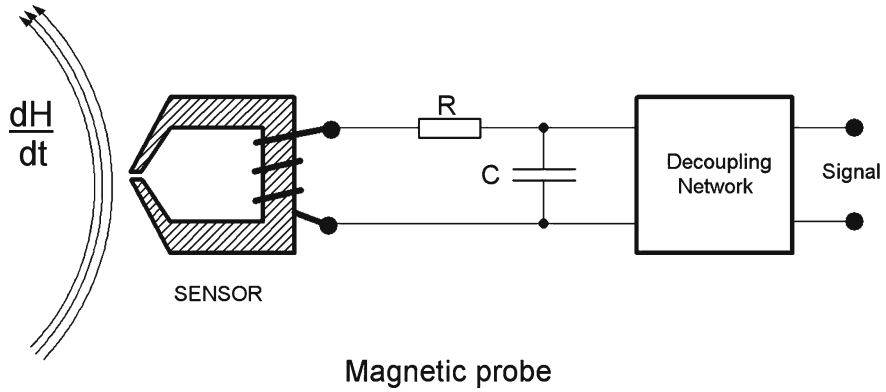

Figure 1. Principle of a coil-based magnetic sensor.

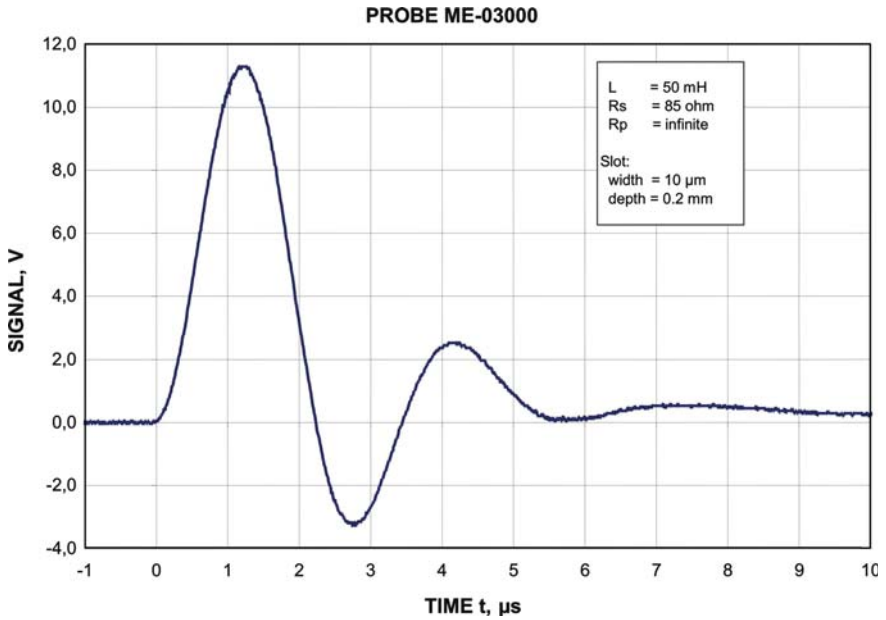

Figure 2. Characteristic of a magnetic sensor according to Figure 1.

The hitherto used probes consist basically of a coil as the sensor, that is described more realistic by an oscillation circuit (which is unavoidable due to inherent capacitors, resistors, cables, etc.). Figure 1 shows a schematic of this probe. Additionally a decoupling circuit is required so that the unavoidable elements, capacitor and damping resistor, are small or tolerable, but anyway fixed, and the sensor is decoupled from varying external influences. These elements are chosen so that the circuit works close to the critical damping and the sensor's transfer function is similar to a differential signal. Figure 2 shows the response of a probe to a jump function of the magnetic field, this is called the 'characteristic' of the probe.

An example of a non-logarithmic ME signal is shown in Figure 3. A Charpy test was performed with a structural steel showing brittle fracture at room temperature. The upper signal is the uncalibrated force vs. time curve. This curve shows an abrupt force decay after about 265 μs. The sample broke fast and separated completely, and

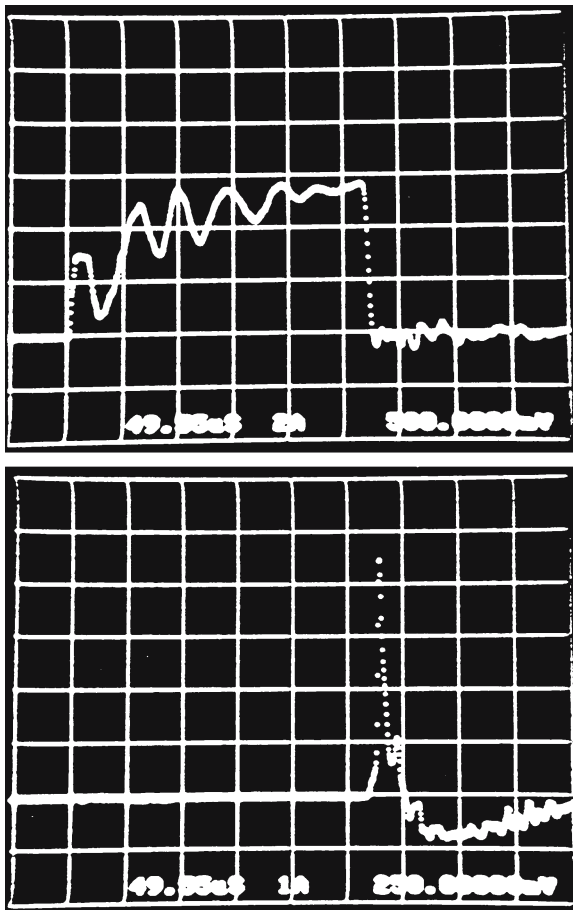

Figure 3. Charpy test with a brittle material; time axes: 50 μs/div. (Upper graph) force curve 0.5 V/div; (Lower graph) ME signal, 0.25 V/div.

the force remains at zero after fracture. Just some hits with the moving halves of the sample are registered thereafter. The lower curve is the corresponding ME signal. A large peak, >1V, at the instant of the force drop indicates fast brittle fracture. This signal shows more clearly than the force signal that the fracture begins relatively slowly but then speeds up (0.5 μs is the oscilloscope's sample rate). The ME behavior thereafter indicates the movements of the sample halves that carry their magnetic field with them.

Such ME signals can easily serve as trigger signals for force and displacement registration in pre-triggered monitoring. They are the fastest signals in a brittle fracture experiment and have successfully been applied as trigger signals in, for instance, tensile tests where catching the signals is much more difficult than in Charpy experiments.

An experiment on a material that does not fracture in a brittle manner yielded the uncalibrated force curve and the logarithmic ME signal (lower curve) shown in Figure 4. The force curve gives almost no hints of fracture. While the linear ME signal showed few features, the log (ME) signal indicates the beginning of the wave effects in the sample with a peak of about 10 mV and at the maximum load the

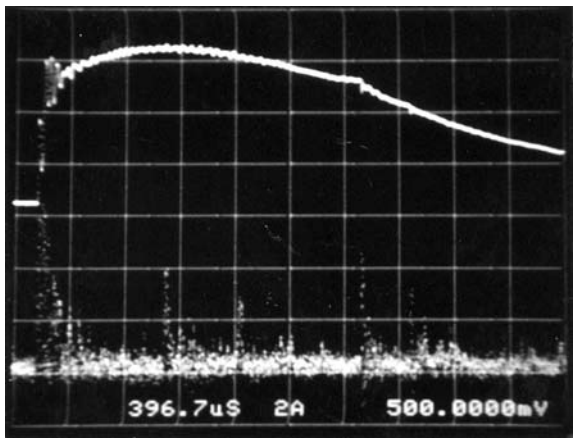

Figure 4. Charpy test with ductile material behavior, time axis 400 μs/div; (Upper graph) force, 0.5 V/div; (Lower graph) log(ME), 0.5 decades/div; noise level $\approx$0.4 mV, the first peak is about 10 mV.

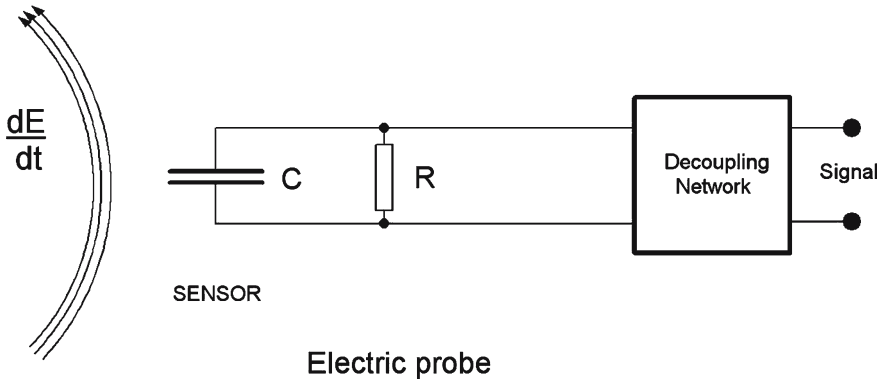

Figure 5. Principle of a capacitor-based electric sensor.

first fracture signals that seem to repeat in certain intervals (amplitude $\sim$3 mV). This example shows that ME pinpoints the onset of fracture and provides some details of the discontinuous fracture progress.

3. Electric emission (EE)

The origin of an electric field produced by mechanical stress or damage depends on the material. An electric field can be caused by deformed molecules or microstructures or by separated charges. Thus, field changes can be produced by elastic or plastic deformations as well as by the generation of new surfaces during fracture. All materials (metals, plastics, glass, wood, etc) seem to show this effect. A more extended investigation of the effect with different materials was carried out by Sklarczyk et al. (1995).

Electric field variations can be picked up by a capacitor. A field E in the vicinity of the capacitor induces a charge q on it which is proportional to the originating electric field. The signal U (the voltage across the capacitor) is given by

$$U = \frac{q}{C}. \tag{4}$$

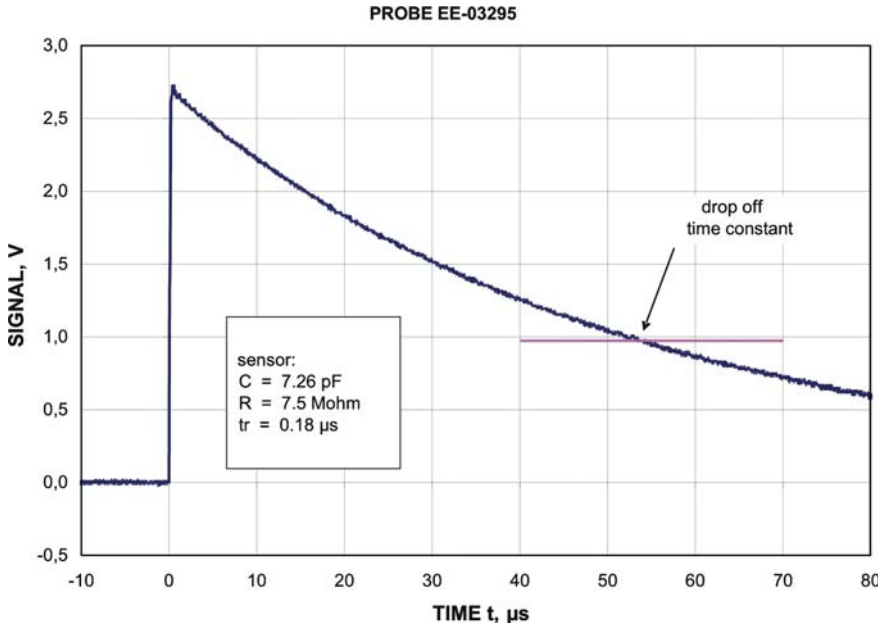

Figure 6. Characteristic of an electric sensor according to Figure 5.

Thus, for a fixed q (i.e., a certain field change), the smaller the capacitance C, the larger is the signal U. A discharging resistor is required in parallel to the capacitor so that this sensor again has a differentiating character. Figure 5 is the schematic of that kind of a probe and Figure 6 shows its characteristic.

This characteristic (response to a field jump) appears as a superposition of two exponential functions, a rising and a dropping one. The rise time of the characteristic of Figure 6 is $0.18\,\mu$s (this corresponds to a time constant $\tau = 0.082\,\mu$s), and the drop-off time constant is $54\,\mu$s. This superposition leads to a certain loss of the maximum amplitude. It can be calculated that a relation of the two time constants of the rising part 1 and the decay part 2 should exceed $\tau_2/\tau_1 = 100$ for a loss of not more than $\approx 5\%$. It has been experienced that a decay time constant of some $10\,\mu$s is suitable. To achieve a very small capacitor in the range of one to ten picofarads and to be able to handle this, which is again a decoupling problem, a more sophisticated active decoupling circuit is required.

An example of electric emission due to fracture is the EE signal of a bundle of breaking carbon fibers in a tensile test, Figure 7. This diagram is a certain time window of the entire event showing five breaking fibers. Each peak indicates the fracture of a single fiber. From the rise time t_r of the signal and the rise time $t_{r,1}$ of the characteristic, the rise time $t_{r,2}$ of the breaking fiber ($\approx$ fracture time) can be determined (Winkler, 1991) according to

$$t_r \approx \sqrt{t_{r,1}^2 + t_{r,2}^2}. \tag{5}$$

The difference in the amplitudes of Figure 7 is due to smaller or larger distances of the fibers from the sensor. The diagram also shows a horizontal line for the tensile force of the machine at 0.89 kN. There is no indication at all of these fracture events

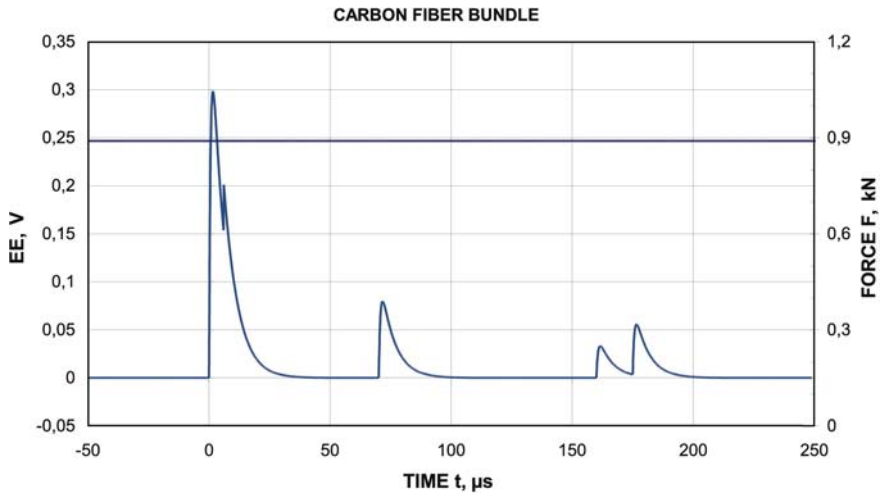

Figure 7. Tensile test with a bundle of carbon fibers. Shown is a part of the EE signal with five broken fibers.

in the force signal which means that most fibers of the bundle consisting of several thousand fibers of 7 μm diameter are still intact. Again, this EE signal appears to be an excellent trigger signal as described before with ME.

Electric emission was also applied in measurements of sound wave propagation velocities in ceramic materials and plastics (Winkler, 1993). This was done with two EE probes. The distance of the two sensors divided by the time difference between the two signals yields the velocity. Slabs of the material were impacted side-on by a bullet ($v_0 \approx 150$ m/s) to produce the mechanical wave. A passing wave obviously leads to structural deformations that give rise to a change of the external electric field and, therefore, can be detected by electric emission sensors.

4. Field considerations

ME and EE are both field emissions which means, no contact is required between sample and sensor. This is in contrast to acoustic emission which needs an excellent contact between sensor and sample. It is also in contrast to electron emission methods investigated by Dickinson et al. (1991 for instance), which require a high vacuum for a sufficient free path length of the emitted electrons.

Field emission sensors, therefore, do not require any sample preparation or even an accurate adjustment – which makes them easy to be applied. The Charpy test is particularly suited to be instrumented by these probes, because they can be affixed to the moving hammer and be at the right place when emission occurs, see Figure 8. In contrast to acoustic emission these field emission methods are also very fast since magnetic and electric fields expand with the speed of light.

It is, however, difficult to predict amplitudes since these depend on the distance between source and sensor and on the field distribution which depends on the shape of the source; a point-like source, for example, can drop off in a squared manner with distance, a line-shaped one linearly. Furthermore, one has to expect sources with shapes and distances varying with time.

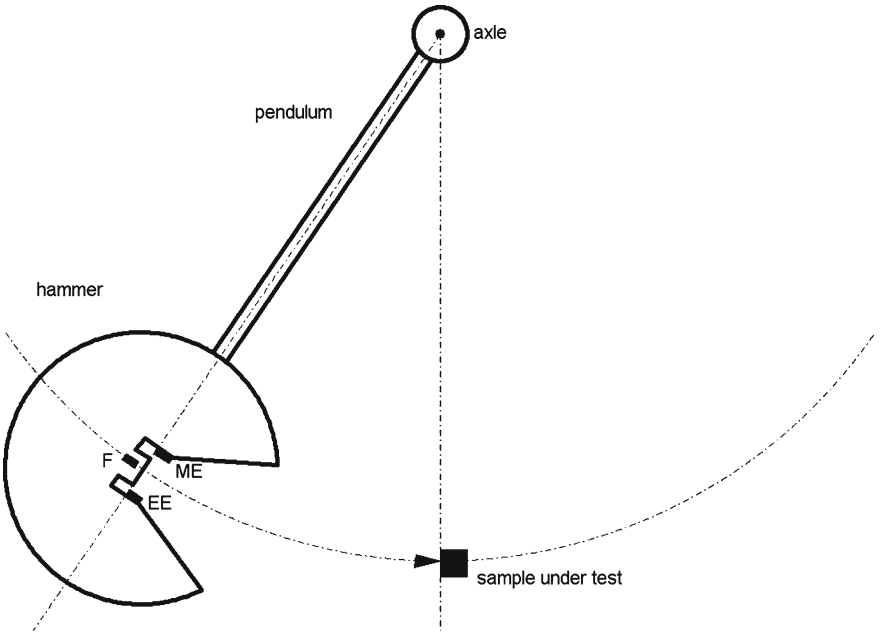

Figure 8. Schematic of an instrumented Charpy hammer.

One of the main goals with ME is to gain the onset of fracture in a fracture mechanics experiment. The problem, however, to temporally localise this event, is obviously difficult with ME if fracture starts with elementary events in subcritical experiments. These signals are often too small to be identified within Barkhausen and electronic noise. There is, however, a possibility to distinguish elementary crack signals from random noise, because the crack originated signals are unipolar and random noise is not. Therefore one is enabled to add them to an increasing (or decreasing) curve. To this end one only needs to integrate the ME curve and the randomly polarized Barkhausen or electronic noise will not contribute to the accumulation of the crack signals. The integrated ME signal, Equation (6), presents a curve that is proportional to the magnetic field, MF, at the place where the sensor is positioned.

$$MF(t) = \int_0^t ME(t')\,\mathrm{d}t' \tag{6}$$

where the unknown (and here of no interest) integration constant – the local static field – has been set to zero. This way one can observe even the otherwise undetectable onset of fracture in sub-critical experiments as the intersection point of the accumulating curve and the flat noise curve. The crack's progress can be followed up by the slope of the curve (Winkler and Winkler, 1998; Winkler et al., 1998). The slope of the field curve indicates the growth of the fracture surface A:

$$\text{Slope} \propto \frac{\mathrm{d}A}{\mathrm{d}t}. \tag{7}$$

It will be shown in Section 6 that also the integrated electric emission, the electric field, EF, offers new insights, even though the reasons for EE are completely different from the magnetic case. This electric field, EF, can be calculated from EE using Equation (6) by replacing the two 'M's by two 'M's.

5. Units

The unit of the magnetic field strength **H** is *A/m*, that of the electric field strength **E** is *V/m* (ASTM E 380 – 76), the units for the magnetic emission (ME) is consequently $[dH/dt] = A/(m \cdot s)$ and $[dE/dt] = V/(m \cdot s)$ for the electric emission (EE).

In practice, however, the basic signals ME and EE appear both as oscilloscope traces, i.e., as calibrated in volts. A recalculation of these quantities in magnetic and electric field units, resp., would be at least difficult if not impossible and with no advantage. It was decided, therefore, for the experiments described here not to use the symbols dH/dt and dE/dt for these quantities but rather ME and EE instead and these be measured in millivolts (mV) and in time units of milliseconds (ms).

The field signals are computed from the signals ME and EE according to Equation (6) by integration. This leads directly to units mV·ms, that is, to μVs. This is the unit used for both the fields. Consequently, it is not talked about field strengths H or E but rather of MF (magnetic field) and EF (electric field) in order to avoid confusion.

6. Combining ME and EE in steel experiments

The application of the two emissions, ME and EE, combined in one test makes sense of course only with ferromagnetic materials, i.e., practically with steel as a test material. This combination of the two methods has been used in Charpy impact tests. Figure 8 shows the principle of a Charpy machine equipped with the sensors. A pendulum-like moving hammer hits the sample. The hammer carries all three probes, one for force *F* and two for emissions ME and EE. It turned out that EE does not react so much on fracture, rather on plastic effects. The dislocation motion during plastic deformation – slip on crystallographic planes – generates charge separation and observable but due to the conductive material short-lived electric fields.

The capability of the combination of the two emission methods shall be demonstrated with a Charpy test on S 460 M structural steel at a striking velocity of 5 m/s. The fracture surface (Figures 9 and 10, two different photos of the same thing) shows a strong plastic behavior: three major plastic events follow a big plastic deformation of the notch tip. The flat parts of the surface are relatively smooth, indicating kind of stable crack propagation. These areas are shrunk by large shear lips.

Three registered signals, force *F*, and emissions ME and EE, shown in Figure 11, are basic for the test evaluation. The diagram of Figure 12, established by a mathematical procedure, shows the loss of speed of the hammer during the test. Two of the three basic curves (Figure 11) appear rather featureless, in particular the smooth force curve. The ME signal indicates that the sample obviously broke more or less continuously with decreasing activities when the force decreases. Only the EE signal shows large activities in the first 1.5 milliseconds.

Figure 9. Test BM5; broken test sample, fracture surface 1.

Figure 10. Test BM5; broken test sample, fracture surface 2.

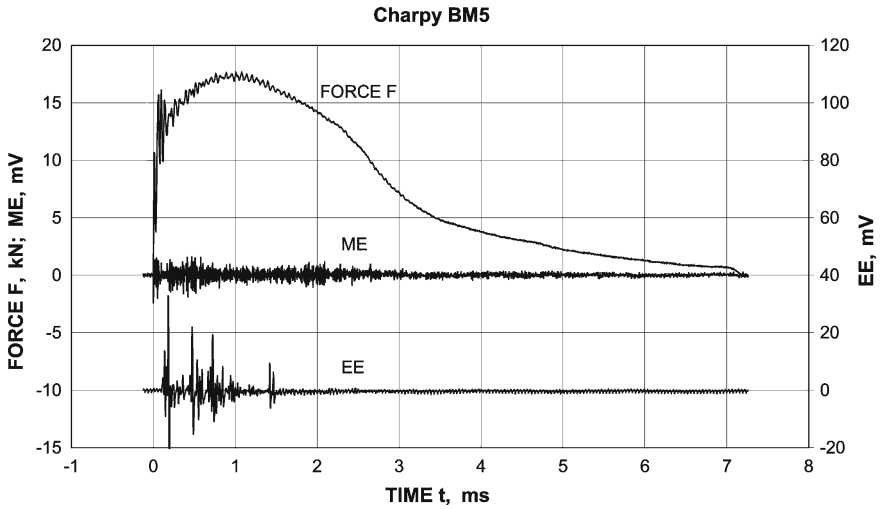

Figure 11. Test BM5; total of the registered signals: Force F, ME, and EE; sample rate 2 μs.

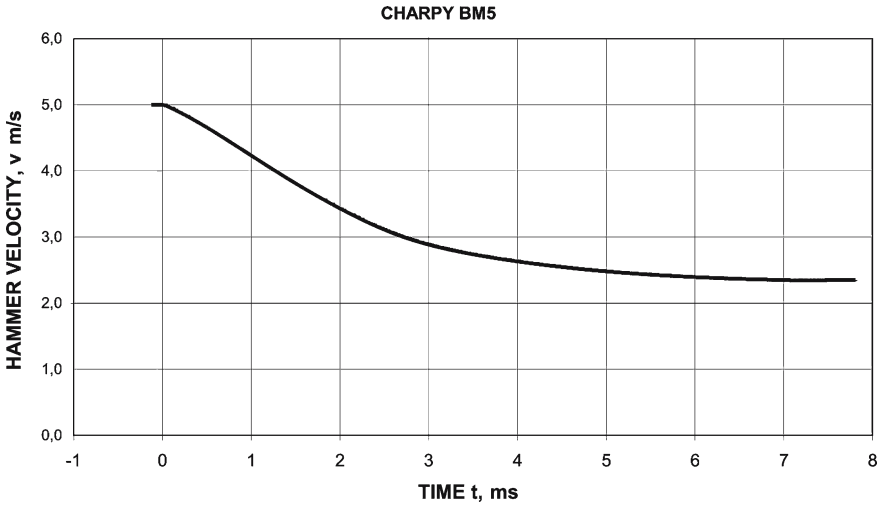

Figure 12. Test BM5; loss of hammer velocity during the test, computed.

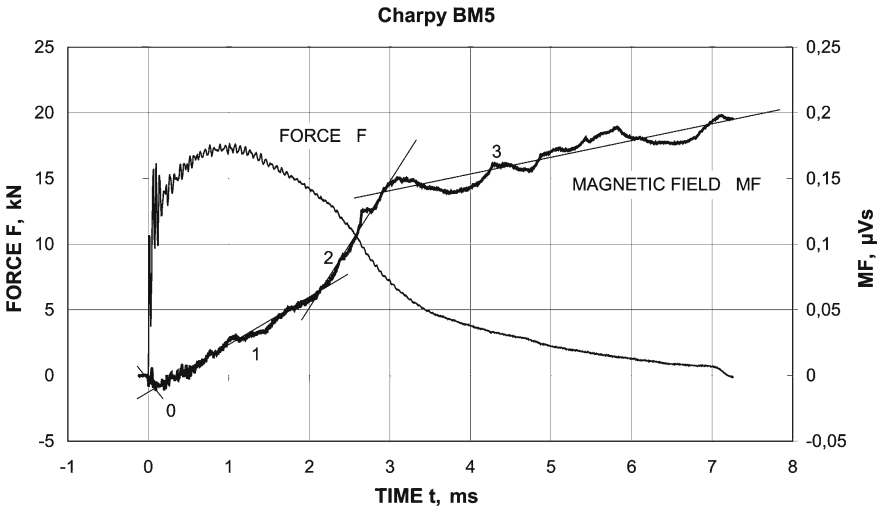

Figure 13. Test BM5; magnetic field vs. time.

The integrated ME signal (Figure 13), i.e., the local magnetic field MF, shows four different main regions as is indicated by the four slopes labelled 0 to 3, and pointed out by inserted straight lines. The slope of region 0 is negative and designates the development of a field due to the irreversible Barkhausen noise caused by impact stress waves: no crack, therefore "0". This changes when fracture occurs indicated by the beginning of region 1. This slope can be correlated to the production of the flat areas between and close to the four 'plastic events'. During the time interval from 2 to 3 ms, when the steeper slope 2 is observed, the subsequent central flat and more rough (i.e. fast crack velocity) area is produced. This crack with slope 2 reduces the strength of the sample drastically so that the force drops to $\approx 1/4$ of its maximum value. With the final slope 3 in the interval from 3 to 7 ms the shear lips, the last weak connection that keeps the two sample halves together, eventually separate. The

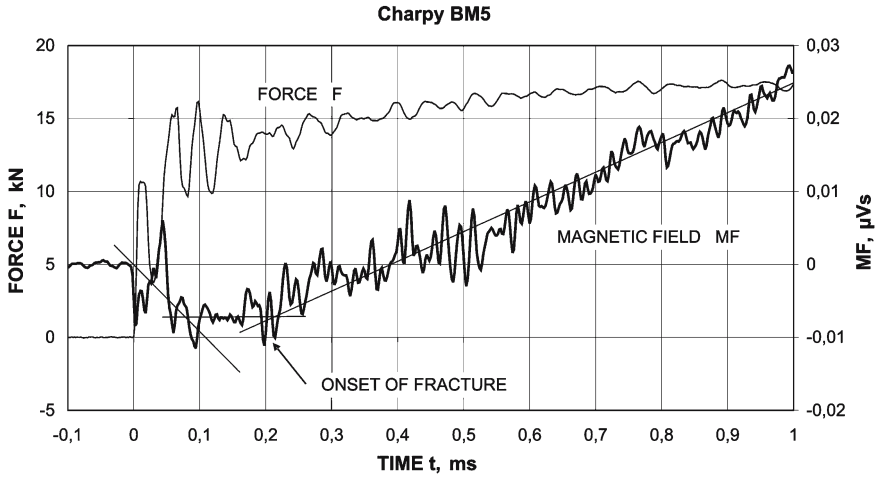

Figure 14. Test BM5; magnetic field at the beginning (ext. of Figure 10).

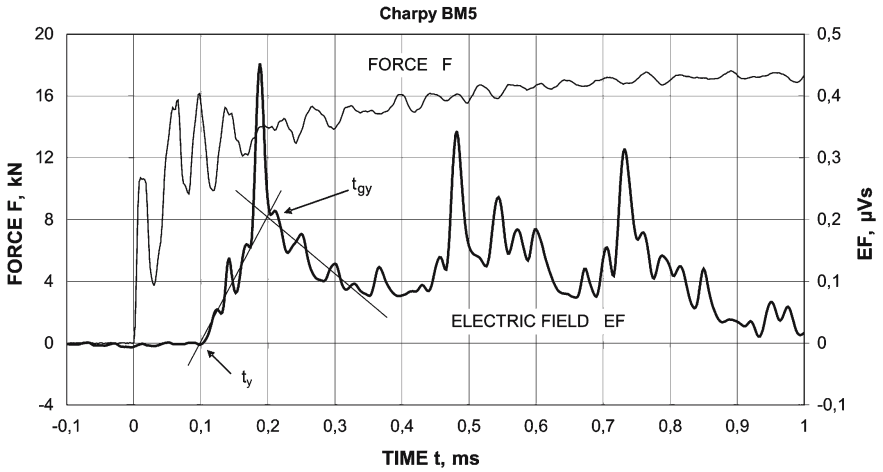

Figure 15. Test BM5; electric field at the beginning.

hammer speed has reduced to ≈ 2.5 m/s, Figure 12, and this is roughly the speed of that crack propagation.

The beginning of fracture is more resolved in Figure 14, an extension of Figure 13. Here the effect of the impact stress waves is more clearly observed with its negative slope within the first 100 μs. This stops for another 100 μs, while nothing seems to happen. And then, at $t \approx 200\,\mu$s, fracture begins and propagates more or less steadily with constant mean speeds.

The electric field signal in Figure 15 tells what happened in that short period of the magnetic stagnation between 0.1 and 0.2 ms. This was the period of plastic deformation of the ligament, beginning in the notch tip. An inserted straight line indicates the rising electric field due to the increasing plastic volume in the sample. The onset of yielding occurs at $t_y = 0.96$ ms, as can be seen in EE (Figure 11) as well as in EF (Figure 15). However, one cannot conclude from the EE signal when general yielding, t_{gy}, occurs, i.e., when the sample's ligament behaves completely plastic. This can

be observed in EF (Figure 15) after the first huge plastic deformation signal (174 – ~ 200 μs) when the field, EF, suddenly decreases at 0.2 ms after its increase. This instant is when general yield, t_{gy}, occurs. The signals EE and EF show four (in Figure 11 and the first three in Figure 15) large plastic events that can be observed on the fracture surface, too (Figures 9 and 10). The first event is obviously the gross notch tip deformation that begins at 174 μs and ends at $\approx$200 μs. The three other plastic events occur at 480, 730, and 1420 μs. It seems that there is no relationship between the magnitudes of the signals to the size of the surface events. But this appears plausible if it is considered that the EE sensor (right side position in Figure 10) sees less of the signals of the larger objects number 2 and 4 (counted from the notch tip) than the closer object number 3 which seems smaller.

These results are remarkable. Neither the force curve nor the magnetic emission curve gives any hints of this plastic behavior of the material, but electric emission does! It indicates the four strong plastic events that are evident on the fracture surface. The magnetic emission signal shows nothing of them, only the relatively smooth crack propagation with slightly different mean speeds in the vicinity of the plastic events composed by microscopic details. A comparison of Figure 15 with Figure 14 shows that in MF the first three events are slightly indicated by larger magnetic activities that possibly are due to the generation of relief stress waves and their reflections, since the average field change is zero in these short time intervals of ~100 μs. From this follows that the 'fine structure' of region 1 of the magnetic field (Figures 13 and 14) has a more staircase-like behavior than just a straight uprise.

With the three basic measurements (Figure 11) of an experiment and some calculations one often can constitute or derive the following features or data, or part of them:

(a) the entire behavior of crack development, in general and local,
(b) the onset of fracture,
(c) the relative or absolute speed dA/dt of the generation of fracture surfaces, A,
(d) the relative or even absolute crack speed dc_T/dt – depends on the character of the fracture,
(e) the yielding behavior, in general and local,
(f) the onset of yielding, t_y, and
(g) the instant of general yield, t_{gy}.

7. Conclusions

The experiences of the group of investigators mentioned in the Acknowledgements below over the past 15 years of investigating and applying field emission techniques in hundreds of experiments have been convincing that sensing methods based on ME and EE hold great promise for providing a better understanding of the material's internal events that occur during loading and fracturing. Such methods applied to fracture mechanics tests yield fast, accurate, direct and in some cases heretofore inaccessible measurements of important critical events of crack initiation and yielding in a direct way instead of the currently used indirect conventional methods that need many samples or test series. Convincing is the simplicity of these techniques with no sample preparation or complicated adjustments. Each test delivers its own

accurate data. Although primarily the instants of events (e.g., the onset of a crack) and the relative velocities of crack surface expansions can be determined, amplitudes in similar tests can also be compared. Also the velocities of stress waves caused by an impact in ceramic and plastic slabs have successfully been determined by two EE probes at a certain distance. Present day sensors seem to have reached a certain maturity, but new sensors based on effects such as EE and ME discussed here could expand and extend current abilities to monitor and measure material response.

Acknowledgements

Thanks are owed to the Fraunhofer Institut für Werkstoffmechanik, Freiburg, Germany, where most of this work was done over the last 15 or more years. I am thankful for all the support from the institute, in particular from Dr. J.G. Blauel, regarding this work while being employed there and still in occasional work after my retirement, and for the encouragement while preparing this paper. Thanks also to Dr. Gyöngyvér B. Lenkey, deputy director of the Bay Zoltán Institute in Miskolctapolca and associate professor of the University of Miskolc, Hungary, who has always trusted in these novel techniques and successfully performed – and performs still – experiments in her laboratory. I enjoyed an excellent and fruitful cooperation in a three-year European contract (EU supported German-Hungarian cooperation contract) with the results being published in reports, journal articles, and conference proceedings with some examples listed in the References: Lenkeyné and Winkler (1995, 1996, 1997) and Lenkeyné et al. (1995a,b, 1996).

References

see for example: ASTM E380 – 76, Standard for Metric Practice, and: DIN 1324 – 88 Elektromagnetisches Feld – Teil 1: Zustandsgrößen (in German).

Barkhausen, H. (1919). Zwei mit Hilfe der neuen Verstärker entdeckte Erscheinungen, Physik. Zeitschr. XX, S. 401–403 (in German).

Dickinson, J.T., Jensen, L. and Jahan-Latibari, A. (1984). Fracto-emission: The role of charge separation, *Journal of Vaccum Science and Technology* **A2**, 1112–1116.

Kittel, Ch. (1986). *Introduction to Solid State Physics*, 6th edn., J. Wiley & Sons, Inc., New York.

Lenkeyné, Gy. B. and Winkler, S. (1995). On the applicability of the magnetic emission technique for the determination of ductile crack initiation in impact tests, Proceedings of the 7th International Conference on Mechanical Behaviour of Materials, ICM 7, pp. 381–382, The Hague, The Netherlands, May 28–June 2, 1995.

Lenkeyné, Gy. B. and Winkler, S. (1996/1). A mágneses és elektro-emissziós méréstechnika alkalmazása műszerezett űtővizsgálatnál, *Anyagvizsgálók Lapja*, pp. 14–16, (in Hungarian)

Lenkeyné, Gy. B. and Winkler, S. (1997) On the applicability of the magnetic emission technique for the determination of ductile crack initiation in impact tests, *Journal of Fatigue Fracture Engineering in Material Structure* **20**(2), 143–150.

Lenkeyné, Gy. B., Winkler, S. and Tóth, L. (1995a). Mágneses és elektro-emissziós méréstechnika alkalmazása műszerezett űtővizsgálattal, Proceedings of the Micro Cad 95, pp. 118–123, Miskolc, Hungary, February 21–24, 1995a (in Hungarian).

Lenkeyné, Gy. B., Winkler, S. and Tóth, L. (1995b) A reperdésterjedés körülményeinek viszgálata mágneses és elektroemissziós méréstechnikával műszerezett űtővizsgálatnál, Proceedings of the V. Törésmechanikai Szeminárium (Vth Hungarian Seminar on Fracture Mechanics), pp. 256–265, Miskolc-Tapolca, Hungary, April 3–6, 1995 (in Hungarian).

Lenkeyné, Gy. B., Winkler, S., Major, Z. and Lévay, I. (1996). Applicability of magnetic and electric emission techniques for detecting crack initiation, Proceedings of the 11th European Conference on Fracture, ECF 11, Vol III, pp. 2025–2034, Poitiers, France, September 3–6, 1996.

Sklarczyk, C., Altpeter, I., Winkler, S. and Thielicke, B. (1995). Grundlagenuntersuchungen zur Elektrischen Emission zur Erkennung wachsender Schädigungen insbesondere in Faserverbundwerkstoffen sowie zur berührungslosen Detektion von Schallwellen an dielektrischen Oberflächen, IzfP-Bericht 950129-TW (in German).

Winkler, S. (1988). Magnetische Emission, ein neues Brucherkennungsverfahren, Fraunhofer-IWM-Bericht T 3/88 (in German).

Winkler, S. (1990a). Brucherkennung mit elektrischer Emission, Fraunhofer-IWM-Bericht T 10/90 (in German).

Winkler, S.R. (1990b). Magnetic emission detection of crack Initiation, in ASTM STP 1074, Gudas, J. P., Joyce, J. A. and Hackett, E. M. (eds), *American Society for Testing and Materials*, Philadelphia, pp. 178–192.

see for instance: Winkler, S. (1991). On the Determination of Dynamic Properties of Instrumentation, Conference on Instrumented Impact Testing of Metallic Materials, National Physical Laboratory (NPL), Teddington, UK, 14–15 November 1991.

Winkler, S. (1993). Experimental Investigation of Wave and Fracture Phenomena in Impacted Ceramics, Experiments on Sapphire, IWM Project 301 388, Final Report, Contract US Army ERO DAJA45-90-C-0053, R&D 6472-MS-01, 27 September 1990, IWM-Bericht T 8/93, May 1993.

Winkler, S. (1997). Investigation of Critical Events During Loading and Fracturing of Samples or Structures Utilizing Magnetic and Electric Emission, Final Report, Contracting period February 1, 1994–January 31, 1997, German-Hungarian EU contract CIPA-CT93-0096, Commission of the European Communities, Brussels, February 1997, IWM-Bericht V 29/97.

Winkler, S., Winkler, W.-D. (1998). Fieldemission in Charpy Tests, Fa. Roell-Amsler-Symposium, Gottmadingen, 5 May 1998.

Winkler, S., Lenkey, Gy. B. and Gregor, M. (1998). Feldemissionen bei unterkritischem Risswachstum, Berichtsband zur 30. Tagung des AK ≫ Bruchvorgänge ≪ in Dresden, S. 141–150, 17–18 February 1998 (in German).